

# Fischer–Tropsch Synthesis with the Use of a Porous Catalyst Packing. Feasibility Study of Performing Multiphase Catalytic Process Using Permeable Composite Monoliths

A. G. SIPATROV, A. A. KHASSIN, T. M. YURIEVA, V. A. KIRILLOV, G. K. CHERMASHENTSEVA and V. N. PARMON

*G. K. Borekov Institute of Catalysis, Siberian Branch of the Russian Academy of Sciences,  
Pr. Akademika Lavrentyeva 5, Novosibirsk 630090 (Russia)*

*E-mail: los@catalysis.nsk.su*

## Abstract

A novel scheme for the organization of the three-phase process has been proposed, basing on a new type of a stochastically organized porous and catalytically active composite monolith (PCM). The high catalyst loading ( $1 \text{ g/cm}^3$ ) and high heat conductivity ( $3 \text{ W/(m K)}$ ) make this new material very attractive for exothermic multiphase processes, *e. g.* for the Fischer–Tropsch synthesis. The possibility of preparing strong PCMs with the permeability of 10–500 mDarcy has been demonstrated. The gas-vapor phase flow through a PCM particle can be performed via transport pores which diameter was measured as 4–10  $\mu\text{m}$ . The pressure drop has been shown to be reasonable for the Fischer–Tropsch synthesis. The effectiveness of the PCM usage at 0.1 MPa, 210 °C has been found to be above 70 %. PCM material was concluded to be the prospective for the Fischer–Tropsch synthesis.

## INTRODUCTION

The conversion of renewable energy sources (in particular, that of biomass) to conventional motor fuels may be performed by the junction of biomass gasification and Fischer–Tropsch synthesis. At present, both stages of the process are in the focus of numerous studies [1, 2]. Using the biomass as a raw material lays some specific constrains on the Fischer–Tropsch technology which are mainly related to a comparatively small scale of production. The traditionally proposed slurry bed or monolith trickle-bed reactors are characterized by a high extent of the catalyst dilution (by slurry filling or by monolith block). Thus, the productivity of the reactor volume unit is low leading to high capital costs of the process. The operation of the “small” scale plants using these types of reactors seems to be not self-supporting. Therefore, the challenge is to design a new type of the Fischer–Tropsch three-phase reactor which should combine the advantages of the slurry

bed and trickle-bed reactors (isothermal catalyst bed, high rates of mass transfer) with the high concentration of the catalytically active substance in the reactor volume [3].

It is noteworthy that the high concentration of the active component loading must not be accompanied by the decrease of:

- catalyst bed heat conductivity (isothermal catalyst bed is important for retaining high selectivity of the process, see *e. g.* [4]);
- gas-liquid interface specific area;
- internal diffusion rates inside the porous structure of a catalyst grain (it is important not only for providing a high effectiveness factor of the catalyst usage but also for ensuring a high selectivity of the process [5]);
- hydraulic permeability of the catalyst bed.

Only in case that all above criteria are maintained at the highest level, the increase of the catalyst concentration in the reactor volume can lead to a better process performance.

Here we present an experimental study on the possibility of providing the Fischer–Tropsch

synthesis in a new type of a three-phase reactor which combines the dense catalyst bed and high rates of mass and heat transfer.

**Proposed concept of the porous catalyst packing: Permeable Composite Monolith (PCM)**

The origin of the PCM concept lies in high loading of the active component in the catalyst grain combined with the low void volume in the reactor volume. In this case, an intense mass-transfer can be achieved by directing the gas flow through the catalyst grain via a set of transport pores, provided that the concentration of the transport pores is high enough.

Then, the effective diffusion length will be about the mean distance between the neighboring transport pores. In [5], it was concluded that for a typical Fischer–Tropsch catalyst, internal diffusion constrains do not worsen the process selectivity at the catalyst grain size less than 50  $\mu\text{m}$ . Assuming the close packing of pores, this corresponds to the concentration of the transport pores  $n_{\text{tp}} > 7 \cdot 10^8 \text{ m}^{-2}$ .

A high area of the gas-liquid interface could be created by making the gas flow through the transport pores partially filled by the liquid in the “annular” regime, provided the concentration of such pores is high enough and their effective diameter is quite small. Assuming the mass-transfer coefficient on the gas-liquid boundary,  $k_L$ , to be about  $10^{-4} \text{ m/s}$  (estimated by the Moo – Young equation [6]), the reaction rate to be not higher than 6 mol (CO)/( $\text{m}^3 \text{ s}$ ) (*i. e.* 300 kg/( $\text{m}^3 \text{ h}$ ) of hydrocarbons produced), and solubility of CO in hydrocarbons to be about 52 mol (CO)/( $\text{m}^3 \text{ MPa}$ ) (measured for octacosane,  $T = 250 \text{ }^\circ\text{C}$  [7]), one can estimate that the specific area of the gas-liquid interface should be above  $20 \text{ cm}^2/\text{cm}^3$  to relax the mass-transfer restrictions at the interface for the typical Fischer–Tropsch conditions (2 MPa, 33 % of CO).

At the same time, the effective radius of the transport pores should be high enough to provide a low pressure drop. Let us estimate the minimal permeability (the Darcy’s law coefficient) of a PCM grain, assuming that the gas feed rate in the industrial Fischer–Tropsch synthesis can hardly exceed  $1 \text{ m}^3/(\text{m}^3 \text{ s})$ , and the

minimal reasonable catalyst bed length is about 0.1 m. Then, the reasonable pressure drop,  $\Delta P < 0.5 \text{ MPa}$ , can be achieved, if the permeability of the catalyst bed is above  $2 \cdot 10^{-14} \text{ m}^2$  (20 mDarcy).

The challenge is to prepare a catalyst grain, which satisfies all the above criteria. We have made an attempt to prepare the catalyst grain using the combination of the state-of-the-art techniques known for the preparation of composite materials. Later we will demonstrate that this attempt has been successful. This new type of catalyst grains we will further denote as “permeable composite monolith” (PCM) catalyst.

**EXPERIMENTAL**

PCM catalyst grains were prepared basing on the Co-containing catalyst. The cobalt loading in the catalyst powder was 24 % mass. The concentration of the catalyst in the PCM samples varied from 0.7 to 1.1 g/ $\text{cm}^3$ . The PCM particles under study have a cylinder geometry with the base diameter of 15 mm and height of 5–7 mm.

Porosity of the PCM samples was calculated by relating the true volume of the catalyst grain to its geometrical volume. The true volume was measured using a Helium picnometer Micromeritics 1320 (USA). Independently, the porosity was estimated by flooding the PCM grain with liquid *n*-tetradecane,  $n\text{-C}_{14}\text{H}_{30}$ , and by comparing the weight of the flooded grain and its initial weight.

Permeability of the PCM samples was estimated by the Darcy equation from the dependence of the pressure drop *versus* the gas flow through the PCM grain at room temperature. The pore size distribution of the PCM samples was estimated by the bubble point method at room temperature using the syngas flow and *n*-tetradecane. Thermal conductivity was evaluated from the experimental data on the electric conductivity by the well-known Wiedemann – Franz correlation [8].

Mechanical strength was taken from experiments when the glass vessel with the catalyst PCM grain was shaken with the frequency of 50 Hz and the amplitude of 5 mm. The PCM sample was free and stroke against the vessel

wall at each oscillation. The weight fraction retained by the PCM sample after 20 min treatment was used as a measure of its mechanical strength. These studies were performed after all the other tests have been over.

The catalytic tests were performed at  $T = 483$  K,  $P = 0.1$  MPa,  $H_2 : CO = 2$  (mol). 10 % vol. of  $N_2$  was introduced into the gas flow as an internal standard for gas chromatography. The gas mixture was saturated by  $n$ -tetradecane vapors (at 483 K) for the uniformity of all the catalytic test series. Thus, the partial pressure of CO in the gas feed was ca. 20 kPa, that of  $H_2$  was ca. 40 kPa.

The PCM samples used in the catalytic tests were sealed into a solid ring to insulate the cylinder element. The PCM sample volume was ca.  $1.05$  cm<sup>3</sup>. The amount of the active catalyst loading varied slightly from 0.9 to 1.03 g per a PCM sample. Before starting the test, the PCM samples were pre-activated (reduced) in a hydrogen flow and placed into liquid  $n$ -tetradecane under the protection of flowing Ar to avoid a contact with air oxygen. Then the sample was moved into a plug-flow reactor with the ascending gas flow.

Two series of tests were made: in a "gas" mode (*i. e.* with no additional liquid hydrocarbon introduced into the reactor volume) and in a "gas-liquid" mode (*i. e.* with having the 1–2 cm layer of liquid  $n$ -tetradecane maintained over the top of the PCM cylinder). Note that for the "gas" test series the PCM sample was initially dried by argon flowing through.

The reference data for the evaluation of the PCM performance were obtained by testing the Co-containing catalyst used for the PCM preparation in a slurry bed reactor ( $n$ -tetradecane as a slurry filling). The sample size was 1.1 g with the catalyst powder particle size less than 0.1 mm. The catalyst was activated in the fluidized-bed reactor and placed into liquid  $n$ -tetradecane under the protection of flowing Ar to avoid a contact with air oxygen.

## RESULTS AND DISCUSSION

### Estimation of integral values for the PCM samples

Figure 1 illustrates that the experimental dependencies of the gas flow through the dry

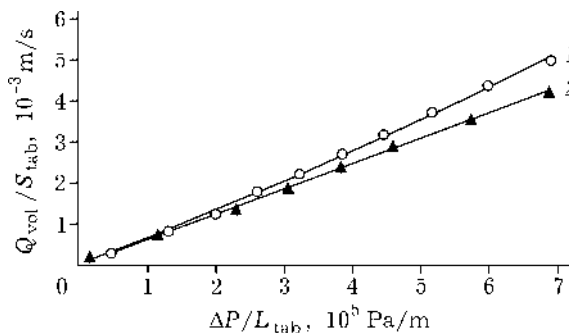


Fig. 1. The experimental data on the dependence of the volume gas flow *versus* the pressure drop for the PCM operated in the "gas" regime: 1 – sample PCM-5; 2 – sample PCM-6.  $T = 22$  °C,  $P = 1$  bar; gas composition: 30 % vol. CO, 60 % vol.  $H_2$  and 10 % vol.  $N_2$ .

PCM grain on the pressure drop follow the Darcy's law for ideal gas:

$$Q_{vol} = K \frac{S}{l\eta} \Delta P \quad (1)$$

Here  $Q_{vol}$  is the volume gas flow, m<sup>3</sup>/s;  $K$  is the PCM permeability, m<sup>2</sup>;  $\eta$  is the dynamic viscosity of gas ( $1.23 \cdot 10^{-5}$  Pa s);  $l$  is the grain height, m;  $\Delta P$  is the pressure drop, Pa;  $S$  is the PCM grain cross-section area, m<sup>2</sup>.

By varying the composition and conditions of the PCM preparation, we found that it was possible to obtain PCM samples which differ a lot by their permeabilities. However, the samples with a higher permeability are less mechanically strong. In Fig. 2 the correlation between these two parameters is shown. It is quite clear from the plot that the PCM grains with the permeabilities,  $K_{gas}$ , ranging from  $10^{-14}$  to

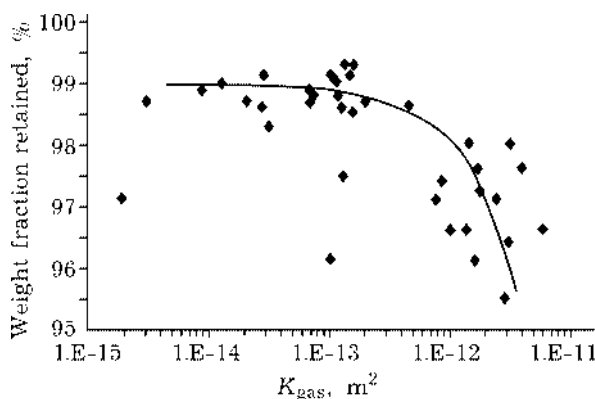


Fig. 2. The correlation of the permeability,  $K_{gas}$ , and the mechanical strength for PCM samples in a wide range of the PCM sample composition and preparation conditions. The mechanical strength is expressed in weight fraction of sample retained after the intense shaking (see the text).

TABLE 1

The experimental data on the PCM samples under study

Sample	Catalyst loading, g/cm <sup>3</sup>	Mechanical strength <sup>a</sup> , %	Porosity <sup>b</sup>	Porosity <sup>c</sup>	Permeability, K <sub>gas</sub> , mDarcy	Heat conductivity, W/(m s)
PCM-1	0.92	98.5	0.64	0.59	120	4
PCM-2	0.99	98.8	0.63	0.56	106	4
PCM-3	0.90	98.7	0.64	0.59	71	3.5
PCM-4	1.04	99.2	0.63	0.59	130	4.5
PCM-5	1.0	98.8	0.56	0.46	75	>5
PCM-6	0.97	98.6	0.64	0.59	158	4

<sup>a</sup>Measured as the weight fraction retained by the sample after 20 min of intense vibrations.<sup>b</sup>Estimated from the true PCM density measured by Helium picnometry.<sup>c</sup>Measured by *n*-tetradecane porometry.

5 10<sup>-13</sup> m<sup>2</sup> (10–500 mDarcy) are optimal. Thus, the scope of the study was confined to a few selected PCM samples with similar preparation conditions and composition.

Table 1 summarizes the experimental data on the catalyst loading, mechanical strength, permeability and thermal conductivity of the selected PCM samples.

#### Estimation of the transport pores distribution by size

Figure 3 represents the effect of the pressure drop on the volume gas flow in the case, when the liquid *n*-tetradecane layer is maintained on the top of the PCM grain (*i. e.* at the “gas-liquid” mode of operation). The data on the PCM-1 sample at 22 °C, *P* = 1 bar were selected for the illustration. It is quite clear that the observed pressure drop originates from the superposition of the capillary pressure and the resistance of a pore to the viscous gas flow:

$$\Delta P = \frac{l\eta}{KS} Q_{\text{vol}} + P_{\text{cap}} \quad (2)$$

and therefore it is not proportional to the gas flow.

At low values of the gas flow, only the widest transport pores are open for the gas flow, *i. e.* those satisfying the necessary condition  $P_{\text{cap}} < \Delta P$ . The observed hysteresis loop indicates the complicated geometry of the pores: the critical value of the pressure drop needed to open a transport pore corresponds to the most narrow spot in the pore, while in decreasing the gas flow the same pore can be

closed only at a somewhat lower pressure drop value equal to the capillary pressure at the pore exit. The experimental dependence  $Q_{\text{vol}}(\Delta P)$  allows us to estimate the density of the transport pore distribution by diameter  $n(D)$  by equation (3):

$$n(D) = \frac{128}{\pi} \left( \frac{4\sigma}{\Delta P} \cos(\Theta) \right)^{-5} \eta l \Delta P \left\{ \frac{P_{\text{atm}}}{\Delta P + P_{\text{atm}}} \times \frac{d^2 Q_{\text{vol}}}{d\Delta P^2} - \frac{P_{\text{atm}}}{(\Delta P + P_{\text{atm}})^2} \frac{dQ_{\text{vol}}}{d\Delta P} \right\}, D = \frac{4\sigma}{\Delta P} \cos(\Theta) \quad (3)$$

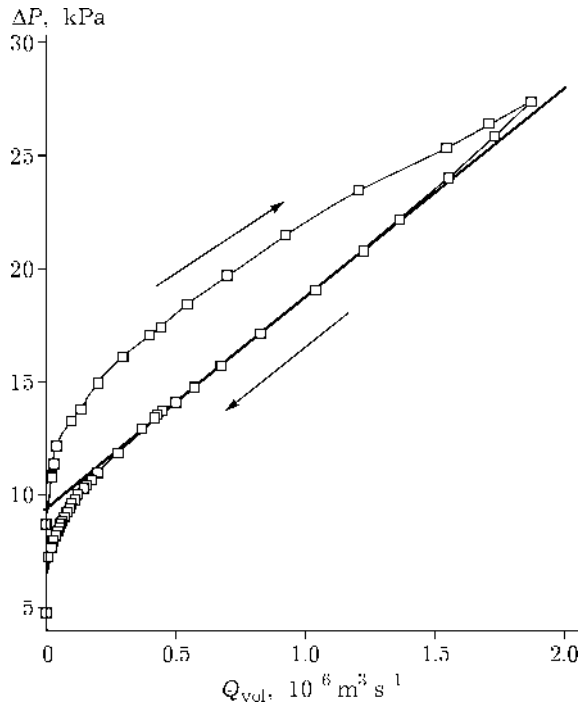


Fig. 3. The experimental dependence of the pressure drop on the volume gas flow for PCM-1 at the “gas-liquid” operation mode.

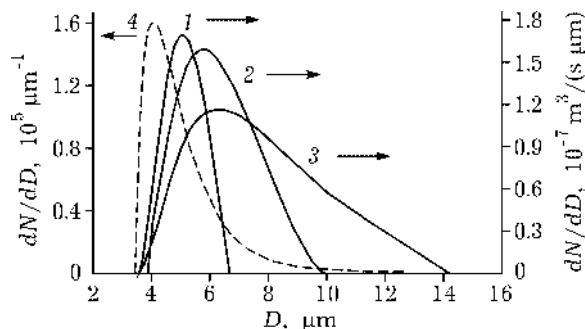


Fig. 4. The estimated density functions of the gas flow distribution by the pore diameter (right axis): 1 - PCM-2; 2 - PCM-3; 3 - PCM-5; and that of the amount of pores distribution by the pore diameter (left axis): 4 - PCM-5.

which follows from eq. (2) and Hagen - Poiseuille equation [9] for the cylindrical pores. In eq. (3),  $\sigma = 2.67 \cdot 10^{-2} \text{ J/m}^2$  is the surface tension of the liquid phase;  $\Theta = 60^\circ$  is the wetting angle;  $D$  is the diameter of the transport pore. A laminar gas flow through the transport pore was assumed. The derivatives,  $\frac{d^2 Q_{\text{vol}}}{d\Delta P^2}$  and  $\frac{dQ_{\text{vol}}}{d\Delta P}$ , were calculated from the 6th degree polynomial approximation of the experimental data on  $Q_{\text{vol}}(\Delta P)$ . The example of the estimated pore distribution density,  $n(D)$ , is presented in Fig. 4 (curve 4).

Curves 1, 2 and 3 in Fig. 4 correspond to the calculated densities of the gas flow distribution by the transport pore size  $\frac{dQ(D)}{dD}$  at the value of  $\Delta P = 15 \text{ kPa}$ :

$$\frac{dQ(D)}{dD} = n(D) \frac{\pi D^4}{128 \ln} \left( \Delta P - \frac{4\sigma \cos(\Theta)}{D} \right) \times \left( 1 + \frac{1}{2P_{\text{atm}}} \left( \Delta P - \frac{4\sigma \cos(\Theta)}{D} \right) \right) \quad (4)$$

TABLE 2

The estimated transport pore structure parameters

Sample	Permeability, $K_{g-1}$ , mDarcy	$R_{\text{tp cap}}$ , $\mu\text{m}$	$R_{\text{tp opt}}$ , $\mu\text{m}$	TP concentration, $n_{\text{tp}}$ , $10^9 \text{ m}^{-2}$	Volume of TP, $\varepsilon_{\text{tp}}$ , %	TP surface area, $a_{\text{tp}}$ , $\text{cm}^2/\text{cm}^3$	Distance TP-TP, $L_{\text{tp}}$ , $\mu\text{m}$
PCM-1	66	3.6	-	1.0	3.6	210	38
PCM-2	30	2.5	2.5	2.7	4.5	370	23
PCM-3	60	3.6	-	1.2	3.6	230	35
PCM-5	53	3.9	5.0	2.0	4.2	320	27
PCM-6	42	3.2	-	2.1	4.3	330	26

The measured values of the PCM permeability  $K_{g-1}$ , estimated transport pores size,  $R_{\text{tp cap}}$ , concentration,  $n_{\text{tp}}$ , volume fraction,  $\varepsilon_{\text{tr}}$ , their specific surface area,  $a_{\text{tp}}$ , as well as the transport pore size measured by optical microscopy,  $R_{\text{tp opt}}$ , are summarized in Table 2.

The permeability,  $K_{g-1}$ , corresponds to the slope of the  $Q_{\text{vol}}(\Delta P)$  plot at  $\Delta P > 15 \text{ kPa}$  (see Fig. 3). The effective size of transport pores,  $R_{\text{tp cap}}$  was estimated by the expression (5):

$$R_{\text{tp cap}} = \frac{1}{2} \int_{D_{\text{min}}}^{D_{\text{max}}} Q'(D) D dD / \int_{D_{\text{min}}}^{D_{\text{max}}} Q'(D) dD \quad (5)$$

where  $Q'(D)$  is the density of the pore size distribution calculated by eq. (4). The concentration of the pores was calculated as the total amount of the pores related to the area of the PCM grain cross-section,  $S$ . Similarly, the volume of the transport pores and their specific surface area were calculated:

$$n_{\text{tp}} = \int_{D_{\text{min}}}^{D_{\text{max}}} n(D) dD / S$$

$$\varepsilon_{\text{tp}} = \int_{D_{\text{min}}}^{D_{\text{max}}} n(D) \frac{\pi D^2}{4} dD / S \quad (6)$$

$$a_{\text{tp}} = \int_{D_{\text{min}}}^{D_{\text{max}}} n(D) \pi D dD / S$$

The data of Tables 1 and 2 indicate that the PCM catalysts satisfy all the requirements postulated in the first section of this article. Thus, it is quite natural to expect their performance to be high. Below, the performance of the PCM catalyst in the Fischer-Tropsch synthesis at  $P = 0.1 \text{ MPa}$  has been discussed.

### Catalytic performance of the PCM samples in CO hydrogenation at 0.1 MPa

The experimental data on the performance of the PCM samples in the Fischer–Tropsch synthesis at 0.1 MPa are summarized in Table 3. Each experimental point refers to 12 h on run at constant reaction conditions for the PCM tests and for 18 h on run for the slurry bed tests.

At the “gas” mode of the operation, the activity of the PCM samples is close to that observed in a slurry reactor over the catalyst powder, *i. e.* under the conditions, when neither internal nor external mass-transfer restrictions can be considered as significant. Thus, almost all the active component particles are

accessible to the gas (the “closed” pores aren’t present in the packing). A high value of propylene-to-propane ratio indicates that the mass-transfer limitations are not strong enough to provide the high probability of a propylene readsorption. On the other hand, the low value of ASF parameter  $\alpha$  for the olefin fraction of the products indicates that for higher olefins a readsorption process is still probable. Some decrease of the  $C_3 =/-$  ratio at the high contact time appears to be a quite expected result: at longer residence time, the probability of propylene readsorption should apparently be higher.

The “gas-liquid” mode of the operation is, probably, closer to the steady-state of the cat-

TABLE 3

The Fischer–Tropsch synthesis performance of the PCM samples in comparison to that of the original catalyst powder in the slurry bed reactor ( $P = 0.1$  MPa,  $H_2 : CO : N_2 = 6 : 3 : 1$ , the  $n\text{-C}_{14}\text{H}_{30}$  saturated vapors)

Sample	T, K	$V_g^a$ , Nl/h	Operation mode	CO conversion, %	Activity, $\mu\text{mol}/(\text{h g}_{\text{cat}})$		Selectivity parameter $\alpha^b$		$C_3 =/-$
					CO converted	$\text{CH}_4$ formed	paraffins	olefins	
SBR	484	0.32	Slurry bed	24	1180	170	0.83	0.80	1.9
	484	0.42		21	1340	180	0.84	0.81	2.0
PCM-2	484	0.94	Gas	11.5	1560	100	0.81	0.59	4.8
	483	0.68		14.6	1570	130	0.80	0.61	4.9
	484	0.46		19.3	1410	130	0.75	0.58	4.6
	484	0.32		25.2	1280	130	0.73	0.56	3.7
	484	0.93	G-L	6.4	940	110	0.79	0.57	3.8
	483	0.67		11.2	1180	140	0.80	0.50	3.3
	484	0.33		21.2	1090	140	0.70	0.41	2.3
	484	0.50		11.6	910	130	0.77	0.54	2.8
PCM-3	483	0.75	Gas	7.6	1050	60	0.84	0.54	5.4
	484	0.31		18.8	1080	120	0.81	0.53	4.9
	484	0.47		13.2	1140	110	0.83	0.56	4.6
	484	0.85	G-L	5.3	820	90	0.78	0.65	4.2
	483	0.34		15.6	950	80	0.81	0.63	2.7
	484	0.50		10.0	880	80	0.80	0.66	3.3
	484	0.50		G-L	11.6	910	130	0.77	0.54
473	0.50	8.8	630		27	0.82	0.75	1.6	
483	0.50	10.6	750		60	0.72	0.74	1.9	
493	0.50	13.2	900		130	0.65	0.63	2.5	
493	0.30	20.1	800	150	0.65	0.63	2.4		
494	0.67	10.1	1030	150	0.67	0.63	3.0		
494	0.91	8.2	1130	150	0.68	0.64	3.4		

<sup>a</sup>The volume flow of the syn-gas before the saturation by the  $n$ -tetradecane vapors.

<sup>b</sup>The values of the Anderson – Schulz – Flory parameter  $\alpha$  are calculated from the composition of  $C_4$ – $C_9$  fraction of corresponding products.

alyst in realistic conditions, when the reaction represents a three-phase process. For this operation mode, the most narrow transport pores are plausibly flooded, *i. e.* “closed” for the gas flow due to the high capillary pressure according to the data of Fig. 3. This provides a less effective usage of the catalyst (60–70 % in respect to the original catalyst powder in the slurry bed reactor).

The propylene-to-propane ratio for the “gas-liquid” operation mode is lower than that for the “gas” mode. This shows that the effective residence time of non-saturated products in the PCM pore structure is higher than the gas residence time due to the existence of additional mass-transfer constrains at the gas-liquid interface. The propylene selectivity in the “gas-liquid” regime seems to be close to the marginal case of a well mixed liquid, when it monotonously increases with the gas velocity. A simple estimation leads to the following equation for the model of gas flowing through the well mixed liquid phase:

$$\left\{ \frac{C_3}{-} \right\}_{\text{observed}} = \left\{ \frac{C_3}{-} \right\} / \left( 1 + \frac{k RT}{V_g P^0} \right) \quad (7)$$

which accords to the experimental data on the PCM samples, provided that  $\left\{ \frac{C_3}{-} \right\} = 6.1$  (see Fig. 5). Here  $\left\{ \frac{C_3}{-} \right\}$  is the rate of the propylene production related to the rate of the propane production (supposing the absence of the re-adsorption);  $V_g$  is the volume gas flow through the PCM grain related to 1 g of the catalyst loading;  $P^0$  is the saturated vapor pressure of propylene;  $k$  is the first order kinetic rate constant for the propylene re-adsorption.

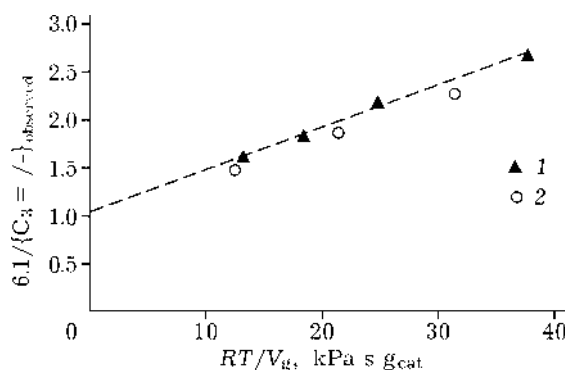


Fig. 5. A linear anamorphism of the impact of the volume gas flow,  $V_g$ , through the PCM-2 (1) and PCM-3 (2) samples on the propylene selectivity.

The above data evidence that mass-transfer constrains are not very severe for the PCM catalysts. Nevertheless, the effectiveness of the catalyst usage in the gas-liquid mode slightly differs for the samples under study. Comparison of the data in Table 3 and those in Fig. 4 reveals, that a wider distribution of pores leads to worse productivity of a PCM sample. The ASF  $\alpha$  parameter is also worse for the PCM-5 sample, when selectivity at a given CO conversion is compared (*e. g.* at 10–12 %). The observed difference may be related with two reasons: (1) the above mentioned flooding of narrow pores make the most narrow pores inaccessible for the gas flow and leads to lower concentration of “active” transport pores in the sample; (2) the contact time of gas is different in wide and narrow pores within the same sample due to difference in hydraulic resistance. Both these reasons are more pronounced for the samples with wider pore distribution leading to worse performance. Therefore, the narrow pore size distribution seems to lead to a better performance.

Despite that, the selectivity towards heavy hydrocarbons (the ASF  $\alpha$  parameter) is quite low at high degree of the CO conversion for the PCM-2 sample, while this tendency. The reason why this tendency is so bright for this particular sample and is not so pronounced for the other two samples is not clear yet and will be under investigation in future.

## CONCLUSIONS

1. In this paper we have demonstrated that it is possible to prepare permeable composite monoliths (PCM) which are characterized by:

- a high concentration of a catalytically active compound (0.9–1.1 g/cm<sup>3</sup>);
- a high heat-conductivity (above 3 W/(m s));
- a high mechanical strength;
- a permeability, which is reasonable for Fischer–Tropsch synthesis ( $10^{-14}$ – $5 \cdot 10^{-13}$  m<sup>2</sup>);
- a well developed transport pore structure with the mean radius of *ca.* 2–5  $\mu$ m and the concentration of *ca.*  $1$ – $3 \cdot 10^9$  m<sup>-2</sup>.

2. The effectiveness factor of the PCM catalyst usage in the three-phase operation mode is enough (60–70 %) to provide the high

productivity of the PCM volume (2–3 times higher, than for the conventional slurry bed reactor). No catalyst is located in the closed pores.

3. Despite the PCM pore structure favors the intense mass-transfer and the mass-transfer restrictions are rather mild, the process performance is sensitive to the mean size of transport pores and to the dispersion of their size distribution. Therefore, studies on the way of the preparation of PCM samples with more homogeneous pore size distribution are necessary.

4. The results of the study encourage us to consider PCM as prospective catalysts for the Fischer–Tropsch synthesis [10], the catalytic tests in more realistic reaction conditions ( $P = 2$  MPa) could give the basis for better-grounded conclusions [11].

### Acknowledgements

We highly appreciate the assistance of Dr. I. Sh. Itenberg. This research is financially supported by grant Copernicus ICAS2–2000–10004 and grant of the Pro-

gramm “Leading Science Schools of Russia” No. 00–15–97446.

### REFERENCES

- 1 M. Kaltschmitt and A. V. Bridgewater (Eds.), Biomass Gasification and Pyrolysis, CPL press, Newbury, UK, 1997.
- 2 H. Schulz, M. Clayes (Eds.), Recent Advances in Fischer–Tropsch Synthesis, *Appl. Catal. A.: Gen.*, 186 (1999).
- 3 A. A. Khassin, V.A. Kirillov, *Kataliz v promyshlennosti (Catalysis in Industry)*, 2 (2002).
- 4 A. A. Khassin, V. A. Parmon, *Dokl. Phys. Chem.*, 368 (4–6) (1999) 283 (Official English translation from Dokl. RAN, 368 (4), 503 (1999)).
- 5 E. Iglesia, *Appl. Catal. A.: Gen.*, 161 (1997) 59.
- 6 P. A. Ramachandran and R. V. Chaudhari, Three-Phase Catalytic Reactors, Gardon and Breach Sci. Publ., New York, 1983.
- 7 C. N. Satterfield, H. G. Stenger, *Ind. Eng. Chem. Processes Des. Dev.*, 24 (1985) 407.
- 8 N. W. Ashcroft, N. D. Mernin, Solid State Physics, Holt, Rinehart&Winston, New York, 1976.
- 9 R. B. Bird, W. E. Stewart, E. N. Lightfoot, Transport Phenomena, Wiley, New York, 2002.
- 10 I. Sh. Itenberg, V. A. Kirillov, N. A. Kuzin *et al.*, Pat. Appl. 2001135572 RU, Priority Date 21.12.2001.
- 11 A. A. Khassin, T. M. Yurieva, A. G. Sipatrov *et al.*, *Catal. Today*, (2003) in press.